Title

Phosphoserine acidic cluster motifs bind distinct basic regions on the μ subunits of clathrin adaptor protein complexes

Journal

Journal of Biological Chemistry, 293(40)

ISSN

0021-9258

Authors

Singh, Rajendra
Stoneham, Charlotte
Lim, Christopher
et al.

Publication Date

2018-10-01

DOI

10.1074/jbc.ra118.003080

Peer reviewed

Phosphoserine acidic cluster motifs bind distinct basic regions on the μ subunits of clathrin adaptor protein complexes

Received for publication, March 22, 2018, and in revised form, August 17, 2018 Published, Papers in Press, August 22, 2018, DOI 10.1074/jbc.RA118.003080

Rajendra Singh[‡1], Charlotte Stoneham[‡], Christopher Lim[§], Xiaofei Jia[¶], Javier Guenaga[‖], Richard Wyatt[‖], Joel O. Wertheim[‡], Yong Xiong[§], and John Guatelli[‡2]**

*From the [‡]Department of Medicine, University of California San Diego, La Jolla, California 92093, the [§]Department of Molecular Biophysics and Biochemistry, Yale University, New Haven, Connecticut 06510, the [¶]Department of Chemistry and Biochemistry, University of Massachusetts, Dartmouth, Massachusetts 02747, the [‖]Department of Immunology and Microbiology, Scripps Research Institute, La Jolla, California 92037, and the **Veterans Affairs San Diego Healthcare System, San Diego, California 92161*

Edited by Charles E. Samuel

Protein trafficking in the endosomal system involves the recognition of specific signals within the cytoplasmic domains (CDs) of transmembrane proteins by clathrin adaptors. One such signal is the phosphoserine acidic cluster (PSAC), the prototype of which is in the endoprotease furin. How PSACs are recognized by clathrin adaptors has been controversial. We reported previously that HIV-1 Vpu, which modulates cellular immunoreceptors, contains a PSAC that binds to the μ subunits of clathrin adaptor protein (AP) complexes. Here, we show that the CD of furin binds the μ subunits of AP-1 and AP-2 in a phosphorylation-dependent manner. Moreover, we identify a potential PSAC in a cytoplasmic loop of the cellular transmembrane Serinc3, an inhibitor of the infectivity of retroviruses. The two serines within the PSAC of Serinc3 are phosphorylated by casein kinase II and mediate interaction with the μ subunits *in vitro*. The sites of these serines vary among mammals in a manner suggesting host–pathogen conflict, yet the Serinc3 PSAC seems dispensable for anti-HIV activity and for counteraction by HIV-1 Nef. The CDs of Vpu and furin and the PSAC-containing loop of Serinc3 each bind the μ subunit of AP-2 (μ2) with similar affinities, but they appear to utilize different basic regions on μ2. The Serinc3 loop requires a region previously reported to bind the acidic plasma membrane lipid phosphatidylinositol 4,5-bisphosphate. These data suggest that the PSACs within different proteins recognize different basic regions on the μ surface, providing the potential to inhibit the activity of viral proteins without necessarily affecting cellular protein trafficking.

Protein sorting within the endosomal system relies in large part on the recognition of short, linear peptide sequences in the cytoplasmic domains of transmembrane proteins (sorting signals) by the coat proteins of transport vesicles (reviewed by Bonifacino and Traub (1)). Heterotetrameric clathrin adaptor protein (AP)[3] complexes (the AP complexes) play a prominent role in this process (reviewed by Robinson (2)). The AP complexes bind both clathrin and various sorting signals (reviewed by Owen *et al.* (3)). The sorting signals are of several types and are commonly tyrosine-based (conforming to the sequence $YXX\phi$, where ϕ denotes a bulky hydrophobic residue) or leucine-based (conforming to the sequence $EXXXL\phi$) or contain phosphoserines flanked by acidic residues (hereafter termed phosphoserine acidic clusters (PSACs)) (1–4).

Whereas the structural basis of how tyrosine- and leucine-based sorting signals bind the AP complexes has been defined (5, 6), how PSAC signals bind is unclear. Certain studies suggest that PSAC sequences, the prototype of which, - SDSEEDE-, is found in the cytoplasmic domain of the endoprotease furin (4), bind to AP complexes via an intermediary adaptor named PACS-1 (7). Others have suggested that these acidic sequences bind directly to the medium-sized (μ) subunit of the AP complexes (8, 9), a compelling notion, given the highly basic nature of the surfaces of the μ subunits (5). In a series of studies culminating in an X-ray crystallographic model, we reported that HIV-1 Nef, a peripheral membrane protein that provides immune evasion by preventing peptide-loaded class I MHC from reaching the cell surface, formed a cooperative ternary complex with the cytoplasmic domain (CD) of the class I MHC α chain and the μ subunit of AP-1 (μ1), a clathrin adaptor involved in transport within the endosomal system (10–12). The interaction of acidic residues both in Nef and in the MHC-I CD with basic regions on μ1 were critical to the formation of this complex; one region (herein basic region 1) participated in a three-way hydrogen-bonding network with residues in both Nef and the MHC-I CD, whereas the other (herein basic region

This work was supported by National Institutes of Health Grants P30 AI036214 (CFAR supplement) (to R. S.), R37 AI081668 and R01 AI129706 (to J. G.), R01 AI102778 (to Y. X.), P01 AI104722 (to R. W.), and K01 AI110181 and R21 AI115701 (to J. O. W.). This work was also supported by the International AIDS Vaccine Initiative (IAVI). The authors declare that they have no conflicts of interest with the contents of this article. The content is solely the responsibility of the authors and does not necessarily represent the official views of the National Institutes of Health.

This article contains supporting Serinc3 sequences used in phylogenetic analysis.

[1] To whom correspondence may be addressed. E-mail: rks003@ucsd.edu.
[2] To whom correspondence may be addressed. E-mail: jguatelli@ucsd.edu.

[3] The abbreviations used are: AP, adaptor protein; PSAC, phosphoserine acidic cluster; MHC, major histocompatibility complex; CD, cytoplasmic domain; CK-II, casein kinase II; MBP, maltose-binding protein; SEC, size-exclusion chromatography; Ni-NTA, nickel-nitrilotriacetic acid; GST, glutathione *S*-transferase; GAPDH, glyceraldehyde-3-phosphate dehydrogenase; L1–L12, loops 1–12; PDB, Protein Data Bank; PIP_2, phosphatidylinositol 4,5-bisphosphate.

2) appeared to provide an electrostatic interaction with an acidic cluster (four consecutive glutamic acid residues) on Nef (12). Notably, the acidic cluster on Nef contains no serines.

Recently, we reported that HIV-1 Vpu, a small transmembrane protein that provides immune evasion by modulating several cellular receptors, including CD4, BST2, NTB-A, and CCR7 (13–16), contains a PSAC of the sequence EDSGNESE in its cytoplasmic domain (17). The serines, when phosphorylated, constitute a phosphodegron that interacts with a β-TrCP–cullin-1 E3 ubiquitin ligase complex (18), but they are also required for a phosphorylation-dependent, direct interaction with both μ1 and μ2 (17); μ2 is the medium subunit of AP-2, a clathrin adaptor that mediates endocytosis (reviewed by Hirst and Robinson (19)). We showed that basic regions 1 and 2 on μ1 were required for the interaction with the Vpu CD, indicating a remarkable convergence in how two viral proteins, Nef and Vpu, co-opt AP-1 (17). Moreover, we showed that the analogous basic regions on μ2 were required for the interaction with Vpu (17).

These results raised the question of whether the CDs of furin and other cellular proteins that contain PSACs also bind directly to μ1 and μ2 and, if so, whether they utilize the same basic regions as Nef and Vpu. Recent data support this notion by showing that the furin PSAC binds to basic region 2 of μ1 (20). Somewhat paradoxically, a μ1 protein in which this basic region is mutated failed to affect the trafficking of furin, a result attributed to the presence of additional, potentially redundant sorting signals in the CD of the protein (20). Whether the furin CD bound μ2 was not tested.

During our study of cellular multipass transmembrane proteins in the Serinc family, some of which inhibit the infectivity of retroviruses, including HIV-1, and are counteracted by Nef (21, 22), we noticed a potential PSAC of sequence SGASDEED in a cytoplasmic loop of Serinc3. Thus, we herein used Serinc3, furin, and Vpu as prototypic as well as novel PSAC-containing viral and cellular proteins to test the hypothesis that PSACs bind to μ subunits at specific basic regions. We found that the CD of furin bound to μ1 and μ2 in a phosphorylation-dependent manner, as did the putative PSAC-containing cytoplasmic loop of Serinc3. Whereas the interaction of the furin CD with μ2 strictly required none of the five individual basic regions tested, the interaction of the Serinc3 loop with μ2 required a basic region previously reported to bind the acidic plasma membrane lipid phosphatidylinositol 4,5-bisphosphate (PIP_2) (reviewed by Jackson *et al.* (23)).

These data suggest that whereas PSACs bind μ subunits, the specific PSACs within different viral and cellular proteins recognize different basic regions on the μ surface. The physiologic relevance of this specificity is not yet clear, but it might provide the opportunity to inhibit the interaction of viral proteins such as Nef and Vpu with the μ subunits without inhibiting the interaction of at least some cellular proteins, such as furin and Serinc3. Finally, we show that the PSAC in Serinc3 has varied considerably during the evolution of placental mammals, specifically at the sites of the key serines, which appear to have co-evolved in a manner consistent with their joint contribution to μ binding. Because such positive selection is often indicative of a virus–host conflict (reviewed by Daugherty and Malik (24)), we speculate that the μ-binding activity of Serinc3 might have varied over the course of evolution in response to the presence or absence of retroviruses that, like HIV-1, encode Serinc antagonists.

Results

Phosphorylation-dependent binding of the cytoplasmic domains of furin and Serinc3 to the μ subunits of AP-1 and AP-2; Serinc3 contains a potential PSAC-sorting signal

Based on our previous studies of the HIV-1 proteins Nef and Vpu and how these proteins interact with the μ subunits of heterotetrameric clathrin adaptors, we tested the general hypothesis that PSAC-sorting motifs bind directly to the basic regions of μ subunits. To do this, we examined the cellular protein furin, a type I transmembrane protein whose CD contains the canonical PSAC motif SDSDEEDE (4), and Serinc3, a multipass transmembrane protein whose predicted long cytoplasmic loop (herein designated loop 10) contains a similar sequence, SGASDEED. HIV-1 Vpu is a type I transmembrane protein whose PSAC sequence is EDSGNESE (17). The predicted topologies of these three proteins and the sequences of their PSAC-containing CDs are shown in Fig. 1 (*A* and *B*). Potential additional AP-binding motifs are also present in Vpu and furin (17, 25–27); these include the *YXXϕ* sequences that have the potential to bind μ subunits via a well-defined "two prong in socket" mechanism (5). Serines that are either reported or shown herein (Fig. 1*C*) to be phosphorylated by casein kinase II (CK-II) are indicated (28, 29).

We co-expressed each of these CDs as GSH-*S*-transferase (GST) fusion proteins in *Escherichia coli* together with CK-II. We analyzed phospho-GST-Serinc3 loop 10 by LC/MS and identified several peptides that together revealed CK-II–mediated phosphorylation at positions 367, 380, 383, and 404 (Fig. 1*C*); serines 380 and 383 are part of the putative PSAC. We analyzed all of the GST-CD fusion proteins (GST-Serinc3 loop 10, GST-Vpu CD, and GST-furin CD) by Phos-tag stain, and each was phosphorylated by CK-II (Fig. 1*D*).

To study the interactions of these phosphorylated CDs with the μ subunits, we used fusions of the C-terminal two-thirds of μ1 or μ2 to maltose-binding protein (MBP; a solubility-enhancing tag) in pulldown assays in which the GST-CD fusion proteins were the bait (Fig. 1, *E* and *F*). Similar to our findings using the same assay to study the CD of Vpu, the CD of furin and loop 10 of Serinc3 each bound to μ1 and μ2 in a CK-II–dependent manner, which presumably reflected the requirement for serine or threonine phosphorylation.

Each of the two phosphoserines of the Serinc3 PSAC contributes to binding

We next used the GST pulldown assay to identify the requirements within Serinc3 loop 10 for binding to the μ subunits (Fig. 2). These requirements were similar for μ1 and μ2 (Fig. 2, *A*, *C*, and *D*). Substitution of both Ser-380 and Ser-383 with asparagines reduced μ binding to the residual levels of the nonphosphorylated protein. Serines 380 and 383 were each individually important, but Ser-383 was the more critical residue for binding to μ2. Binding to μ2 was substantial when Ser-383 was substituted with aspartate, but only when the protein

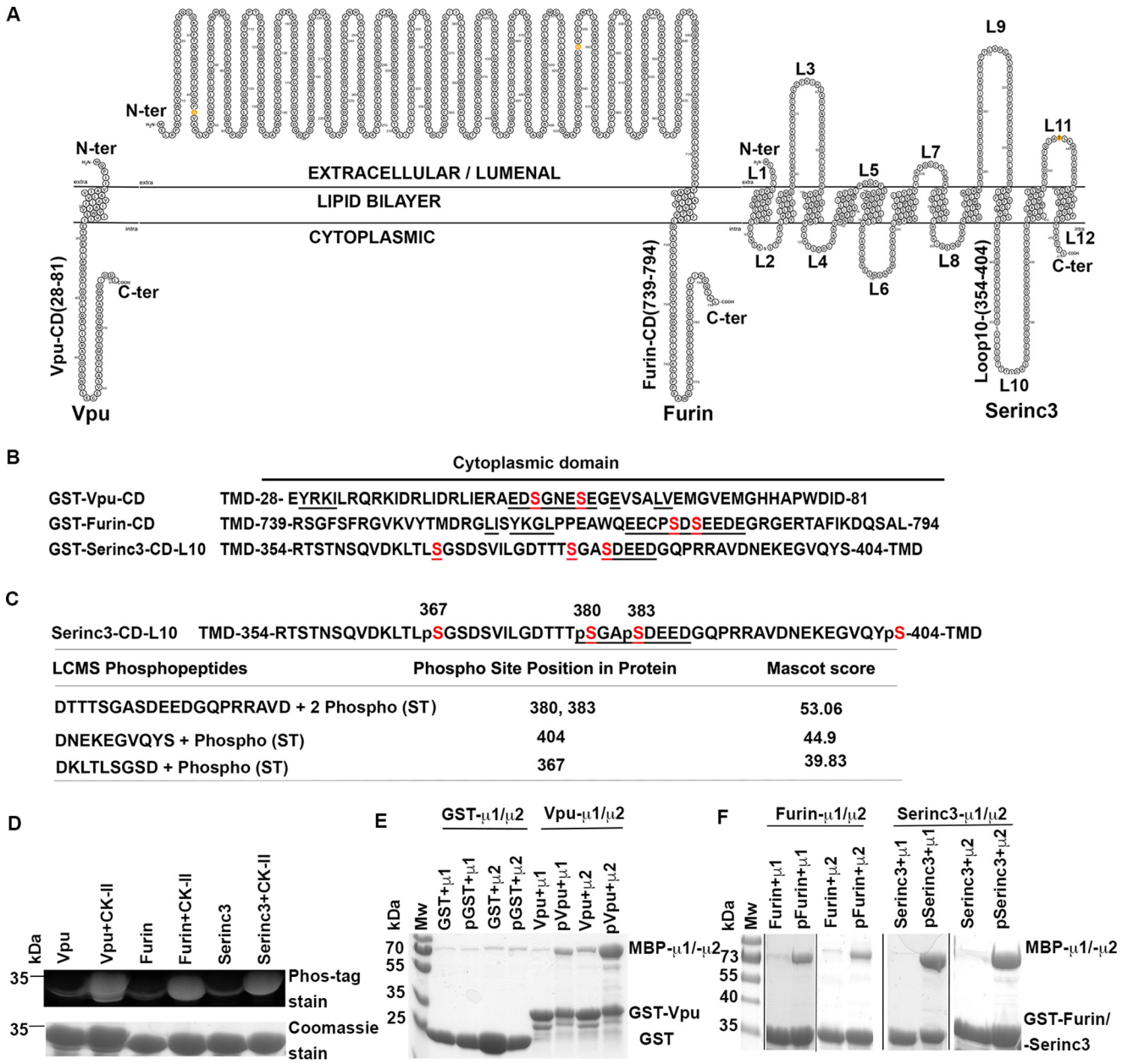

Figure 1. Cytoplasmic domains containing PSACs bind directly to the μ subunits of AP-1 and AP-2. *A*, diagram of the transmembrane proteins HIV-1 Vpu, furin, and Serinc3. Vpu and furin are single-pass, type I transmembrane proteins. Serinc3 is a multipass transmembrane protein. Extracellular/luminal and cytoplasmic regions (loops) of Serinc3 are numbered N-terminally to C-terminally as L1–L12. L10 contains a potential PSAC. *B*, CDs of Vpu and furin and L10 of Serinc3. *TMD*, transmembrane domain. Potential clathrin AP complex–binding motifs, including PSACs, are *underlined*. Serines in *red* are known or potential sites of phosphorylation by CK-II. *C*, sites of serine phosphorylation in L10 of Serinc3. GST-Serinc3-L10 was co-expressed with CK-II in *E. coli*, purified, and analyzed by LC/MS. Phosphopeptides and serine-threonine (*ST*) phosphorylation are indicated, as are the sites of phosphorylation. Mascot scores for the peptide matches are indicated. *D*, phosphorylation of the CDs of Vpu and furin and L10 of Serinc3 detected by Phos-tag staining. GST-Vpu CD, GST-furin CD, or GST-Serinc3-L10 was expressed in *E. coli* either with or without co-expression of CK-II. The proteins were purified by affinity chromatography using GSH-Sepharose, ion-exchange, and size-exclusion chromatography and then stained with either Phos-tag stain or Coomassie Blue. *E*, Vpu binds μ1 and μ2 in a CK-II–dependent manner. GST or GST-Vpu proteins expressed in *E. coli* either with or without CK-II were tested for binding to μ1 and μ2 in a pulldown assay; proteins co-expressed with CK-II are denoted by *p* for presumed phosphorylation. The μ proteins are N-terminally truncated and fused to MBP as a solubility tag. SDS-polyacrylamide gels were stained with Coomassie Blue. *F*, the CD of furin and L10 of Serinc3 bind μ1 and μ2 in a CK-II–dependent manner. GST-furin CD or GST-Serinc3-L10 was expressed either with or without CK-II (proteins co-expressed with CK-II are denoted by *p*). The purified proteins were then used to capture either μ1 or μ2. SDS-polyacrylamide gels were stained with Coomassie Blue.

was phosphorylated (Fig. 2, *A* and *D*); these observations suggested that whereas negative charge is a key attribute required for binding, residues in addition to Ser-383, such as Ser-380, likely require phosphorylation for the loop to bind μ2. Notably, the S383D mutant bound μ1 relatively poorly, even when the protein was phosphorylated (Fig. 2*A*). Fig. 2 (*B* and *E*) shows a reversed pulldown design in which the C-terminal two-thirds of μ2 is used as the bait; the data confirm that Ser-380 and Ser-383 in loop 10 are required for the interaction and further show that serines 356, 359, 367, and 371 are dispensable. Finally, Fig. 2*F* shows that the interaction between Serinc3 loop 10 and μ2 requires the acidic residues DEED within the puta-

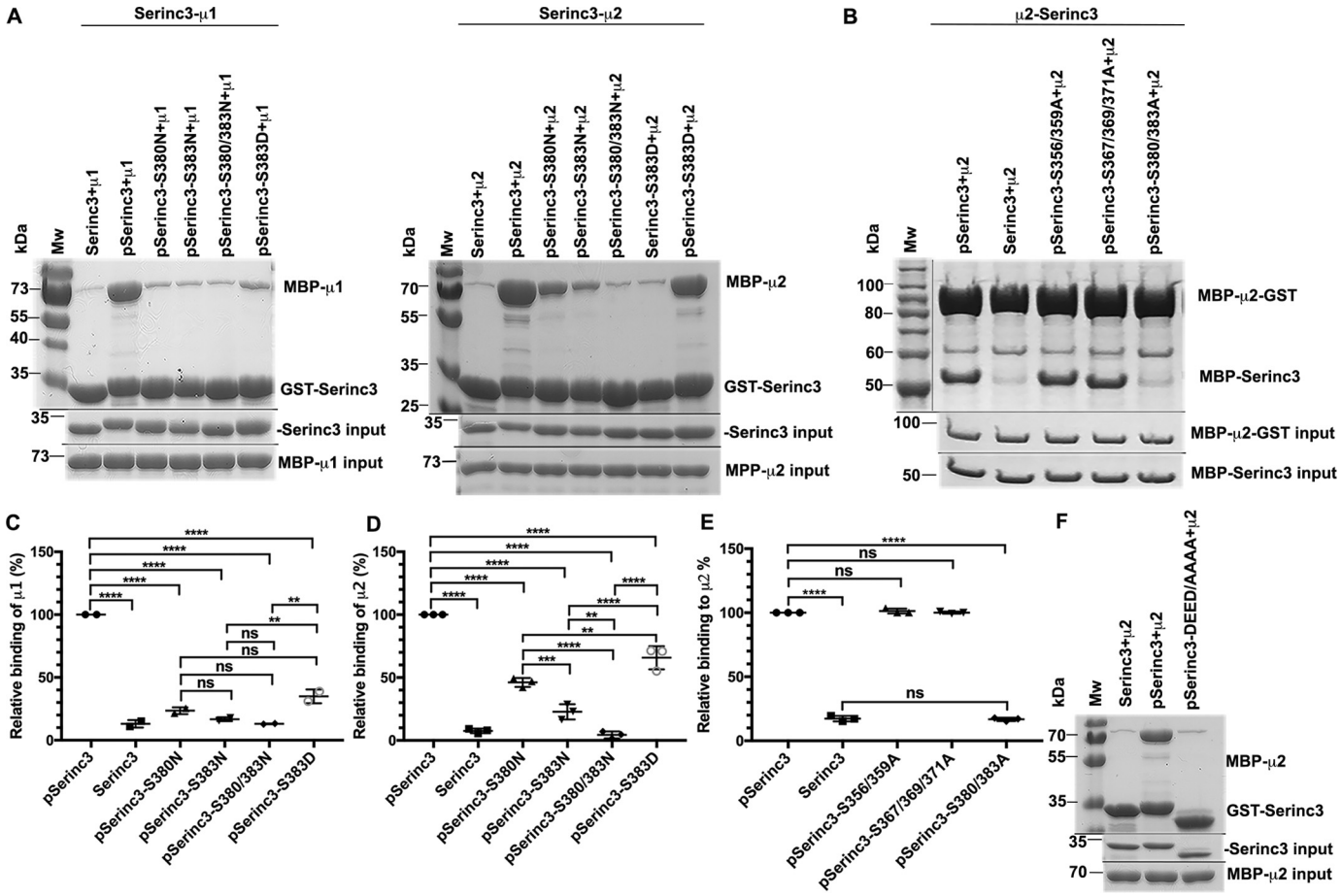

Figure 2. Mutational analysis of the PSAC of Serinc3-L10 with respect to μ-binding. *A*, GST-Serinc3-L10 or the indicated Ser/Asn or Ser/Asp substitution mutants were expressed in *E. coli* either with (*p*) or without (*no p*) co-expression of CK-II; the purified proteins were used to pull down MBP-μ1 or MBP-μ2. *B*, MBP-μ2-GST was used to pull down phospho-MBP-Serinc3-L10. This "reverse" pulldown relative to *A* confirmed the key roles of Ser-380 and Ser-383 in the interaction, and it indicated that Ser-356, Ser-359, Ser-367, Ser-369, and Ser-371 are dispensable. *C*, binding of GST-Serinc3-L10 or related mutants to MBP-μ1 was quantified by band densitometry in duplicate experiments. Values are expressed relative to WT phospho-Serinc3-μ1, which was set at 100%. Individual data points are shown. *Error bars*, S.D. One-way analysis of variance followed by multiple comparisons using Tukey's post hoc test were done using GraphPad Prism version 7 software. Statistically significant differences between the binding of various Serinc3 mutants to μ1 are indicated: ****, $p < 0.0001$; **, $p < 0.0054$. *ns*, nonsignificant differences. *D*, binding of GST-Serinc3-L10 or related mutants to μ2 was quantified by band densitometry in triplicate experiments. Values are expressed relative to WT phospho-Serinc3-μ2, which was set at 100%. Individual data points are shown. *Error bars*, S.D. Statistical analyses were done as above: ****, $p < 0.0001$; ***, $p = 0.0009$; **, $p < 0.0065$. *E*, binding of MBP-μ2-GST to MBP-Serinc3-L10 was quantified by band densitometry in triplicate experiments. Statistical analyses were done as above. *F*, binding of WT Serinc3-L10 or a ^{384}DEED/AAAA mutant to μ2; mutation of the acidic residues abrogates the interaction.

tive PSAC; this might be due to the loss of net negative charge and/or the loss of a sequence recognized by CK-II.

The cytoplasmic domains of Vpu, furin, or Serinc3 cytoplasmic loop 10 form stable complexes with μ2 at submicromolar affinity

We next sought to confirm that the interactions between the CDs of Vpu, furin, and Serinc3 loop 10 with μ2 were stable and to define their kinetics and affinities. We used size-exclusion chromatography (SEC) to analyze equimolar mixtures of the GST fusion proteins containing the CDs of Vpu or furin or Serinc3 loop 10 and MBP-μ2 (Fig. 3*A*). The data indicate that each of these CDs forms stable complexes with μ2, indicated in each case by the peak in the elution profile designated P1.

To define the kinetics and affinities of these interactions, we used biolayer interferometry. We immobilized polyhistidine-tagged MBP-μ2 on a Ni-NTA chip surface and used the GST-CD fusion proteins at different concentrations as the analytes. The association and dissociation steps of the experiments are shown in Fig. 3*B*, and the derived on/off rates and the K_D values for each interaction are shown in Table 1. These data indicated that on rates of the Vpu–μ2, furin–μ2, and Serinc3 loop 10–μ2 interactions are similar, whereas the off rate of the Serinc3 loop 10–μ2 interaction is relatively slow. The K_D values of the Vpu–μ2, furin–μ2, and Serinc3 loop 10–μ2 interactions are all submicromolar. Mutation of Ser-380 and Ser-383 in Serinc3 loop 10 reduced the binding affinity dramatically. The K_D of the furin CD–μ2 interaction, determined here by biolayer interferometry, was 0.46 ± 0.12 μM, substantially less than the published K_D of the interaction of a phosphorylated furin peptide with μ1 determined by isothermal calorimetry (22 μM) or surface plasmon resonance (35 μM) (20). This could reflect differences between μ1 and μ2; the use of a relatively short peptide in the studies of μ1 rather than the entire CD as used here; or the presence of GST tags in our analyte proteins, which could stimulate dimerization and consequently increase the apparent affinity of the CDs for μ2 in the above experiments.

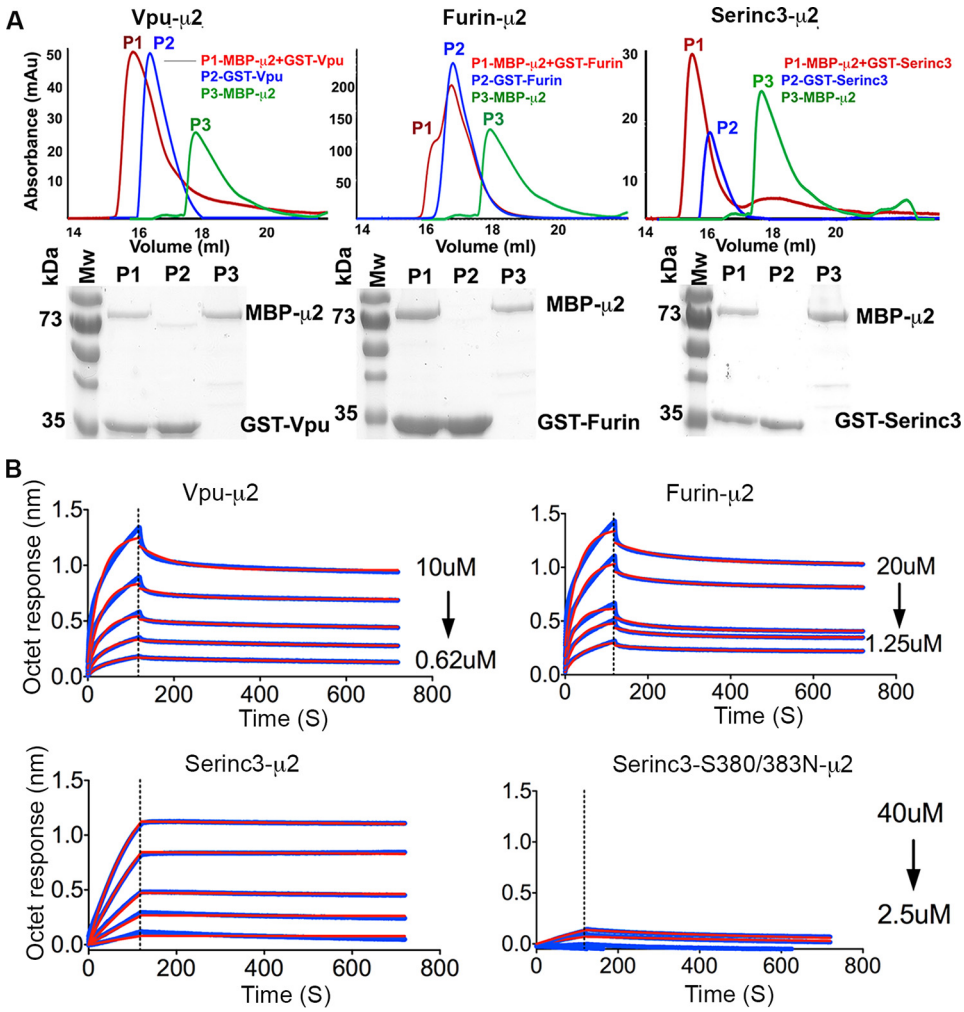

Figure 3. Binding between the Vpu CD, furin CD, or loop 10 of Serinc3 and μ2 measured by SEC and biolayer interferometry. *A*, GST-Vpu CD, GST-furin CD, and GST-Serinc3-L10 were fractionated by SEC either alone (P2; *blue*) or after mixing in equimolar amounts with MBP-μ2 (P1; *red*). MBP-μ2 was also fractionated alone (P3; *green*). *Top*, protein absorbance values *versus* elution volume for the three independent SEC experiments. *Bottom*, Coomassie Blue–stained SDS-polyacrylamide gels of the indicated peaks (P1, P2, and P3). P1 contains the protein complexes. *B*, biolayer interferometry. His-tagged MBP-μ2 was immobilized on a Ni-NTA chip surface; GST-Vpu CD, GST-furin CD, GST-Serinc3-L10, and the GST-Serinc3-L10 S380N/383N mutant were used as analytes at the indicated concentrations. The *vertical dotted lines* separate the association (*left*) from the dissociation (*right*) steps of the experiments. The calculated dissociation constants (K_D) and the on- and off-rates for the interactions are shown in Table 1.

Table 1

K_D, on rate (k_{on}), and off rate (k_{off}) of the interaction of μ2 with PSAC-containing cytoplasmic domains

	K_D[a]	k_{on}[a]	k_{off}[a]
	μM	$M^{-1}\ s^{-1}$	s^{-1}
Vpu-μ2[b]	0.35 ± 0.16	(1.39 ± 0.39) × 10^4	(4.0 ± 0.09) × 10^{-3}
Furin-μ2[c]	0.46 ± 0.12	(1.44 ± 0.25) × 10^4	(6.1 ± 0.10) × 10^{-3}
Serinc3-μ2[d]	0.2 ± 0.041	(3.4 ± 1.08) × 10^4	(0.79 ± 0.4) × 10^{-3}
Serinc3-S380N/383N mutant-μ2[e]	100 ± 77	(2.3 ± 1.5) × 10	(1.15 ± 0.22) × 10^{-3}

[a] Values are the mean ±S.E.
[b] Values are from the binding runs shown in Fig. 3.
[c] Values are from the binding runs shown in Fig. 3 plus a second set of runs using the same protein preparations.
[d] Values are from the binding runs shown in Fig. 3 plus a second set of runs using an independent protein preparation of GST-Serinc3-loop 10.
[e] Values are from the binding runs shown in Fig. 3.

Basic domains on the μ subunits: Serinc3 loop 10 requires basic region 4 for binding, a region previously reported to bind PIP_2

We next sought to map the basic regions on the surface of the μ2 subunit that contribute to the binding of these PSAC-containing CDs. Fig. 4*A* shows a surface representation of μ1 (basic regions in *blue*) complexed to a fusion protein consisting of the CD of the MHC-I α-chain fused to HIV-1 Nef (*red ribbon* and *red space-fill*). This previously published crystal structure led to our identification of two basic regions on μ1, herein designated 1 and 2, that are required for the interaction with MHC-I-Nef (12). Some but not all of the charged lysine and arginine residues in these regions are conserved (see Fig. 4*D*, which shows a structure-based alignment of μ1 and μ2). The analogous basic regions (1 and 2) are indicated on a surface representation of μ2 (Fig. 4*B*); note that basic region 1 of μ2 contains a lysine analogous to arginine 225 of μ1, but it is an unstructured region not shown in Fig. 4*B*. Also note that basic region 2 of μ2 consists of only two lysine residues (Lys-308 and Lys-312); residues analogous to Lys-274 and Arg-303 of μ1 are not present. We recently showed that basic regions 1 and 2 are each required for the binding of the Vpu CD to either μ1 or μ2 (17). We extended this analysis to the interactions of μ2 with the furin CD and loop 10 of Serinc3 (Fig. 4*E*); the pulldown data indicate that neither basic region 1 nor 2 of μ2 is required for the interactions,

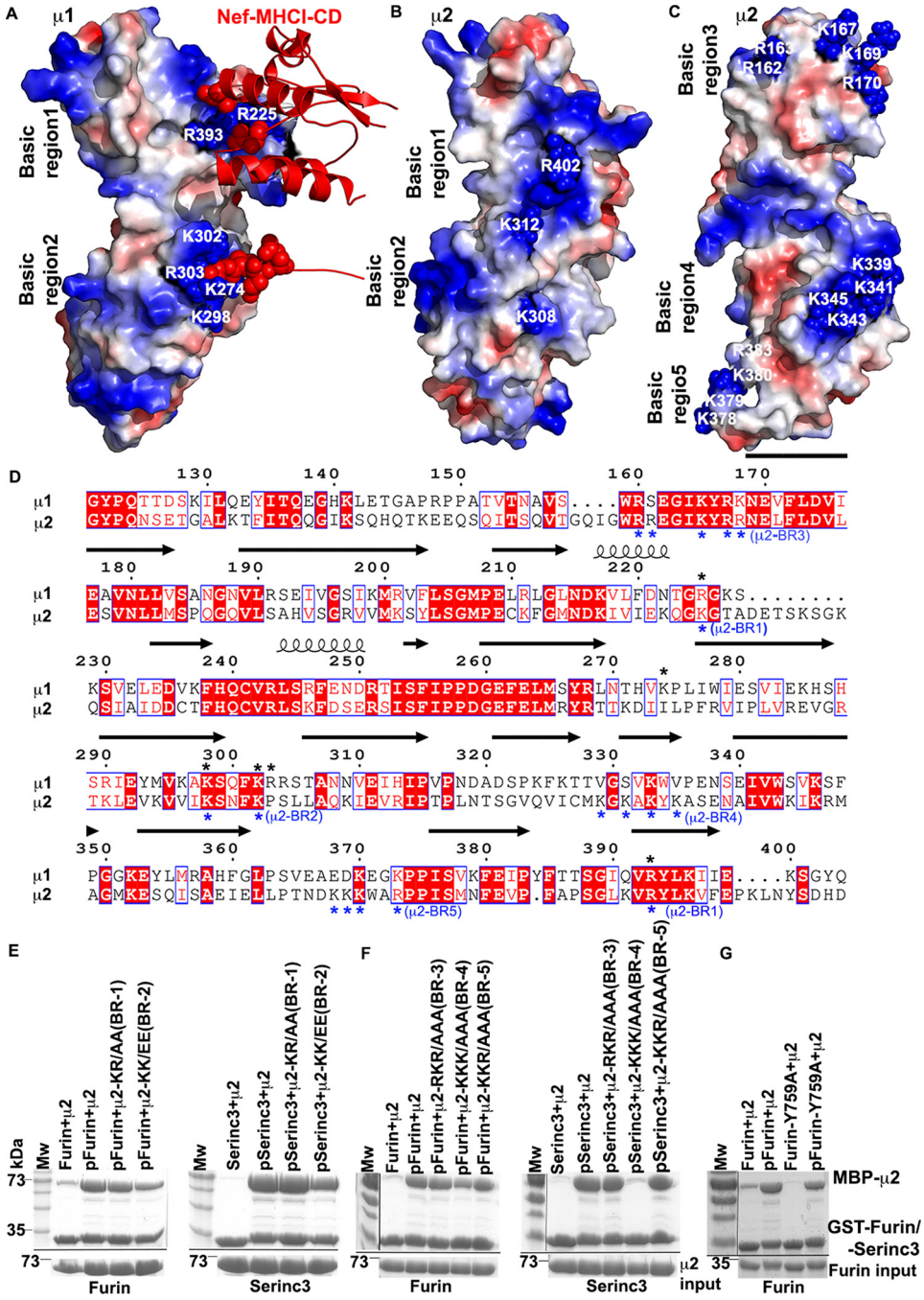

Figure 4. Identification of basic patches on μ2 and their roles in binding the CD of furin and loop 10 of Serinc3. *A*, surface representation of the C-terminal two-thirds of μ1 complexed with HIV-1 Nef fused to the CD of the class I MHC α chain (*red ribbon*; *red space-fill* for the Nef acidic cluster) (PDB code 4EN2). Basic regions (*blue*) 1 and 2 (*numbered residues*) were shown previously to be essential for the interaction. *B*, *surface representation* of μ2 (PDB code 1BW8) with basic regions analogous to regions 1 and 2 of μ1. *C*, *surface representation* of μ2 rotated relative to *B* and indicating additional basic regions 3, 4, and 5. Region 4 is a binding site for the acidic membrane lipid PIP_2. *D*, structure-based sequence alignment of μ1 and μ2 was done using ESPript3 (49). *Black asterisks*, positions of residues constituting basic regions 1 and 2 of μ1. *Blue asterisks*, basic regions 1–5 of μ2. Secondary structures are indicated by *arrows* (β-stands) and coils (α-helices) *above* the *sequence*. *Red boxes* indicate strict identity. *E*, pulldown of MBP-μ2 or the indicated basic region (*BR*) mutants by GST-furin CD or GST-Serinc3-L10. *p*, co-expression of the GST fusion proteins with CK-II. Neither basic region 1 nor 2 of μ2 is required for binding. *F*, pulldown of MBP-μ2 or the indicated basic region mutants by GST-furin CD or GST-Serinc3-L10. Basic region 4 (*BR-4*) is required for binding Serinc3-L10. *G*, pulldown of MBP-μ2 by GST-furin CD or a *YXXϕ* mutant of the furin CD (Y759A). Tyr-759 is required for the phosphorylation-independent binding of the furin CD to μ2 but contributes minimally to the binding of the phosphorylated furin CD.

although basic region 2 might be contributing given the slightly reduced signal.

Given these results, we defined and mutated three additional basic regions on the surface of μ2, designated 3, 4, and 5 and shown in Fig. 4*C* in a surface representation of μ2 that is rotated relative to the view shown in Fig. 4*B*. The roles of these basic regions in the interactions of μ2 with the furin CD and loop 10 of Serinc3 were tested in pulldown assays (Fig. 4*F*); the data indicated that basic regions 3 and 5 are dispensable for these interactions, whereas basic region 4 is required for the binding

of Serinc3 loop 10 and might contribute slightly to the binding of the furin CD. Overall, these data indicate that the furin CD and loop 10 of Serinc3 bind μ2 with requirements for basic regions on the μ-surface different from those we previously defined for Vpu. Whereas the binding of furin persisted despite mutation of any of five different basic regions, binding of loop 10 of Serinc3 required basic region 4, which has been reported previously as a binding site for the plasma membrane–specific phospholipid PIP_2 (30, 31).

Because none of the five basic regions on μ2 were critical for interacting with the furin, we tested the possibility that residual binding was due to the Y*XXϕ* sequence (^{759}YKGL) upstream of the furin PSAC (see Fig. 1*B*) (8). Fig. 4*G* shows that, whereas the residual binding of the furin CD to μ2 in the absence of phosphorylation depended on Tyr-759, the Y759A substitution only minimally decreased binding to μ2 when the furin CD was phosphorylated. These data indicate that the persistent binding of the WT phosphorylated furin CD to the single-basic region μ-mutants shown in Fig. 4 (*E* and *F*) is not attributable to the activity of the Y*XXϕ* sequence.

Genetic variation in the Serinc3 PSAC suggests the possibility of host–pathogen conflict

We previously noted that the sites of Ser-380 and Ser-383 in Serinc3 are under positive (diversifying) selection among primates (32). In some cases, the 383 position is substituted with asparagine, which as shown in Fig. 2 is highly detrimental to μ binding. Here, we examined more completely how this position has varied among placental mammals. A phylogeny of eutheria based on *serinc3* mRNA sequence (see supporting material) is shown in Fig. 5; the branches with amino acid substitutions at position 380 and 383 are *color-coded* (*blue*, 380; *red*, 383; *purple*, 380 and 383). Position 383 of Serinc3 has alternated between serine, asparagine, and glycine during eutherian evolution. Of the 36 nonsynonymous substitutions we detected at these sites across the phylogeny, 32 involved substitutions to or from a serine (Fig. 5). Positions 380 and 383 tend to co-evolve (probability = 0.999 in the Bayesian graphical model), favoring a model in which the amino acid at site 383 is conditionally dependent on the amino acid at site 380. In general, position 380 has evolved toward serine, whereas position 383 has repeatedly evolved away from serine. Nonetheless, the phylogeny indicates four acquisitions of serine at position 383. These results are consistent with the joint contribution of the two serines to μ-binding and indicate that the ability of loop 10 of Serinc3 to bind μ subunits has waxed and waned among placental mammals. This variation could relate to some form of selective pressure, conceivably that of retroviral proteins that counteract the ability of Serinc3 to inhibit infectivity.

The Serinc3 PSAC appears dispensable for the inhibition of HIV-1 infectivity and for counteraction by Nef

Given the forgoing observations, we tested whether the PSAC of Serinc3 affects either its activity in inhibiting viral infectivity or its susceptibility to counteraction by the HIV-1 Nef protein. Insofar as exemplified by Serinc5, Nef reduces the amount of Serinc proteins in virions in a clathrin– and AP-2–dependent manner, thereby counteracting the negative effect of

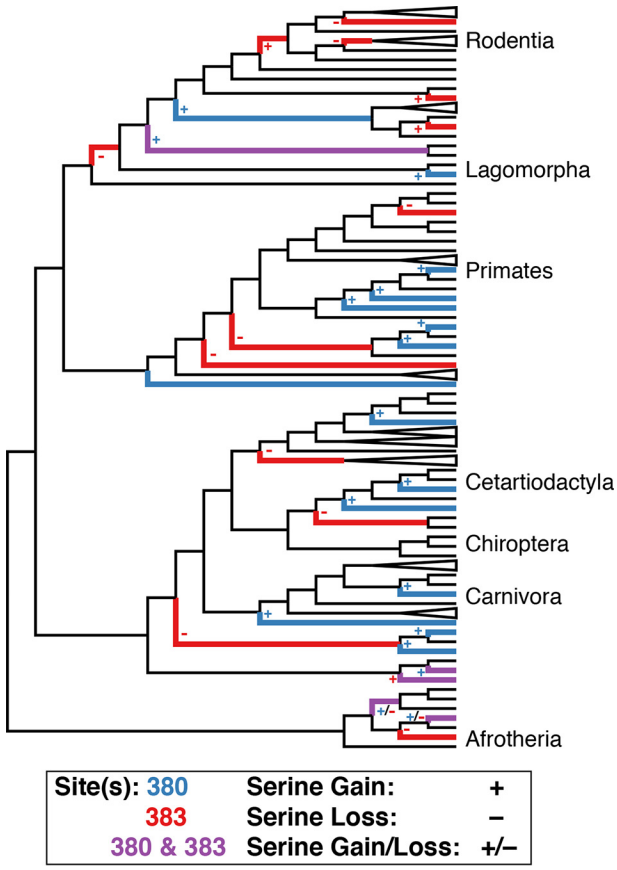

Figure 5. Cladogram of placental mammals depicting the coordinated evolution at codon position 380 and 383 of the Serinc3 loop 10. *Blue branches* indicate amino acid substitutions at site 380, *red branches* indicate amino acid substitutions at 383, and *purple branches* indicate amino acid substitutions at both sites. *Plus signs* indicate a substitution toward serine; *minus signs* indicate a substitution away from serine. The cladogram is based on a maximum likelihood tree of 133 eutherian *serinc3* mRNA sequences. Major mammalian clades are identified.

the Serincs on infectivity (21, 22). We measured the infectivity of HIV-1 virions, either genetically *nef*-positive (WT) or -negative (ΔNef), produced either in the presence or absence of WT Serinc3 or three different PSAC-mutants: a deletion of the sequence SDEED, an alanine substitution mutant of Ser-383, or an alanine substitution mutant of the DEED acidic sequence. Each of the Serinc PSAC mutants inhibited the infectivity of virions produced in the absence of Nef, and each was similarly susceptible to antagonism by Nef (Fig. 6*A*). Western blotting indicated that all of the Serinc3 proteins were detected in partially purified preparations of virions, the apparent site of action of the Serincs (21). Moreover, each of the Serinc3 proteins was excluded from virions by Nef to similar extents. Overall, these data indicate that the Serinc3 PSAC is not a substantial determinant of antiretroviral activity or of the susceptibility of the protein to Nef-mediated antagonism.

Notably, when compared with the WT protein in the absence of Nef, the Serinc3 mutant in which the SDEED sequence was deleted accumulated more efficiently in virions (Fig. 6, *B* and *C*). This observation could be consistent with a reduced rate of Serinc3 endocytosis in the absence of the PSAC, but the ADEED (alanine substitution of Ser-383) and the SAAAA mutations did not show quantitatively similar effects. More-

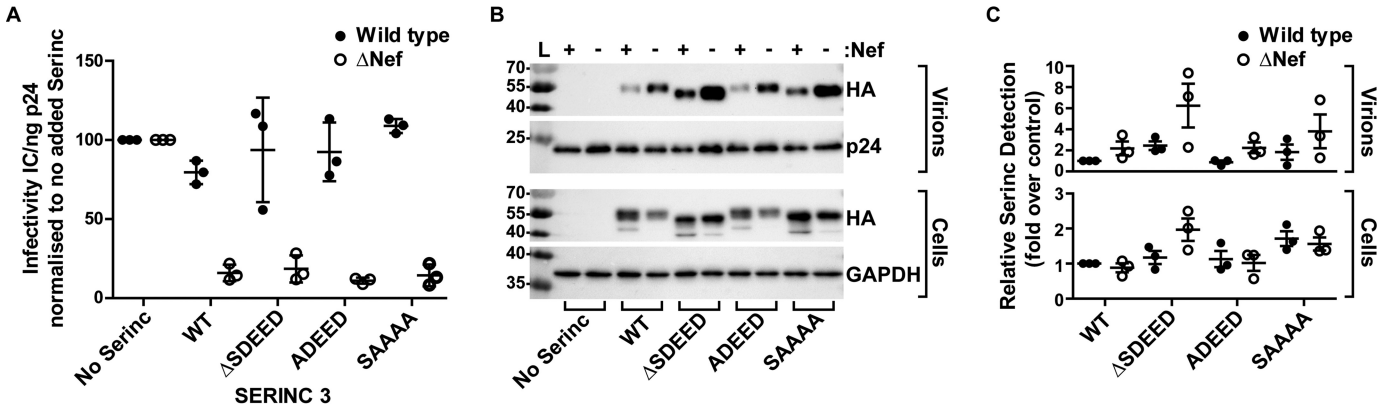

Figure 6. The Serinc3 PSAC is dispensable for antiviral activity and for counteraction by HIV-1 Nef. *A*, WT or *nef*-negative (ΔNef) HIV-1 virions were produced in Jurkat TAg (−*SERINC3*/−*SERINC5*) cells. The cells were co-transfected to express WT or mutant Serinc3 whose PSAC SDEED sequence was either deleted or partially substituted with alanines, as indicated. Viral infectivity was measured in HeLa-CD4 indicator cells; the infectivity (initially calculated as infectious centers (*IC*) per ng of p24 capsid antigen) of each virus (WT or *nef*-negative) in the presence of Serinc3 is expressed relative to its no-Serinc control (set at 100). *Error bars*, S.D. of triplicate, independent experiments. *B*, Western blots of a representative experiment showing Serinc3 (*HA*) in virions (*top*) and virion-producer cells (*bottom*). p24 is the virion-capsid antigen; GAPDH is a cellular protein used as a loading control. *C*, protein band intensities of Serinc3 (HA) and loading controls (p24 or GAPDH) in virions and cells were quantified from three Western blots. Serinc3 protein intensity was normalized to loading controls, and data are expressed relative to the WT HIV-1, WT Serinc3 control (set at 1).

over, the expression of Serinc3 at the cell surface measured by flow cytometry (using a version of the protein containing an HA epitope tag inserted into predicted extracellular loop 9 (Fig. 1*A*)) was unaffected by deletion of the putative PSAC sequence SDEED, and the WT protein was remarkably stable at the cell surface, with less than 25% of surface protein internalized after 10 min (data not shown). These data call into question, at least in the case of overexpressed Serinc3, whether clathrin-mediated endocytosis is a major regulator of surface expression.

Discussion

We tested the hypothesis that the PSAC sorting signals found in the CDs of viral and cellular proteins, here exemplified by HIV-1 Vpu, furin, and Serinc3, bind to specific basic regions on the μ subunits of the clathrin adaptor protein complexes. This hypothesis was initially derived from our identification of two basic regions on μ1 (the μ subunit of AP-1) that interact with acidic residues within the HIV-1 Nef and MHC-I α chain cytoplasmic domain complex (12). It was reinforced by our more recent observation that these basic regions on μ1 and the analogous basic regions on μ2 (the μ subunit of AP-2) are required for interaction with the cytoplasmic domain of the HIV-1 immunomodulatory protein Vpu (17). Thus, we proposed that Vpu contains a PSAC similar to that of the prototypical sequence found in the cellular protein furin (4) and that the cytoplasmic domain of furin might similarly bind the μ subunits via its PSAC.

Here, we found that the CD of furin binds μ1 and μ2 in a phosphorylation-dependent manner. Moreover, we identified a potential PSAC in a cytoplasmic loop of the cellular protein Serinc3, which restricts retroviral infectivity (22). The loop of Serinc3 binds to both μ1 and μ2. We documented that each of the serines in the PSAC of Serinc3 is phosphorylated by casein kinase II *in vitro*, and each contributes to binding to both μ1 and μ2. Whereas the CDs of Vpu, furin, and Serinc3 each bind to μ2 with submicromolar affinity, they appear to interact with different basic regions on the surface of μ2. Remarkably, neither furin nor Serinc3 required either of the basic regions that are utilized by Vpu (17). Serinc3 specifically required a basic region on μ2 that has previously been implicated as a binding site for the acidic phospholipid PIP_2 (23, 30, 31). Moreover, of five basic regions tested on μ2, none were individually required for the interaction with the phosphorylated cytoplasmic domain of furin. These data suggest the possibility of redundancy in the use of specific basic regions by furin and nonoverlapping specificity in the sites recognized by other PSAC-containing CDs, such as those of Vpu and Serinc3.

What could be the biological relevance of multiple binding sites for PSACs on the surface of μ? These multiple sites might provide flexibility for how the PSAC motifs in various CDs can avail themselves of high-affinity binding. For example, this flexibility might allow the PSACs in different proteins to function while at different distances from the membrane, or it might allow the simultaneous use of different types of AP-binding signals within a given protein's CD. Both furin and Vpu, for example, encode potential Y*XXϕ* and E*XXX*L*ϕ* signals at various distances from their PSACs (8, 17, 26, 27). The binding site for Y*XXϕ* signals is, like those for the PSAC signals, on the μ subunits (5). The concomitant recognition of Y*XXϕ* and PSAC signals in the same CD by the μ subunit is plausibly exemplified by the HIV-1 Nef–MHC-I α chain CD–μ1 complex, in which a tyrosine in the MHC-I CD acts as an partial Y*XXϕ* signal and occupies the canonical binding pocket on μ1, whereas acidic residues in Nef and the MHC-I CD (although not PSACs *per se*) simultaneously bind basic regions on the surface of μ1 (12). The tyrosine of the MHC-I CD (Tyr-320) is only seven residues upstream of the aspartate (Asp-327) that binds basic region 1. By analogy, the CD of furin contains a Y*XXϕ* signal whose tyrosine is 10 residues upstream of the closest glutamic acid residue that could contribute to the PSAC; nonetheless, the Y*XXϕ* motif in the furin CD contributed relatively little to the interaction under the conditions tested here, and basic region 1 of μ2 was dispensable. Instead, basic region 2 appeared to contribute modestly to the binding of the furin CD to μ2, a result potentially consistent with the more substantial role reported for this region in binding to μ1 as discussed below (20). Basic

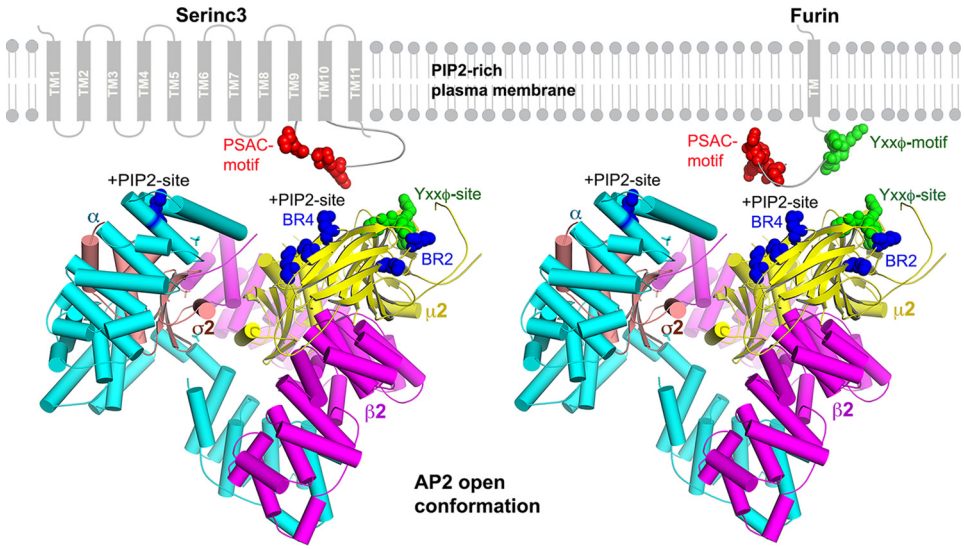

Figure 7. Possible mode of interaction of AP-2 with the PSAC-containing CDs of Serinc3 and furin. The AP2 core is shown in an "open" conformation (PDB code 2XA7) (23). A peptide derived from TGN38 and bound to the *YXXϕ*-binding pocket of μ2 is shown by *green spheres*. Basic regions −2 and −4 are shown by *blue spheres*. Two PIP_2-binding sites on AP-2 are indicated: one on the α subunit and the other on μ2, which is the same as basic region 4. The PIP_2 sites and cargo-binding sites are co-planar and face the membrane. Serinc3 and furin are shown schematically, with the TMs of Serinc3 *numbered;* loop 10, which contains the PSAC, is between TM9 and TM10. PSACs are *red*; *YXXϕ* motifs are *green*. The distances from residue Asp-176 of the *YXXϕ*-binding site to the residues of basic region 4 are 26 Å (to Lys-341), 27.3 Å (to Lys-343), and 30.9 Å (to Lys-345); the distances from Asp-176 to the residues of basic region 2 are 31.8 Å (to Lys-308) and 20.3 Å (to Lys-312). These distances are consistent with simultaneous binding of the furin CD to the *YXXϕ*-binding site via its *YXXϕ* motif and to basic region 4 or 2 via its PSAC.

region 4 also appeared to contribute to the binding of the furin CD to μ2, but its role in binding loop 10 of Serinc3 was much more striking.

How can the Serinc3 PSAC (and perhaps the PSAC in the furin CD) use the basic region on μ2 that has been associated previously with the binding of PIP_2 (30, 31)? Notably, the interaction of AP-2 with PIP_2 is an apparent mechanism by which AP-2 is specifically recruited to the plasma membrane rather than to internal endosomal membranes. At least two binding sites for PIP_2 on AP-2 have been described: one on the μ subunit (herein basic region 4) and another on the larger α subunit (23, 30, 31). These sites have been proposed to act sequentially, with the site on the α subunit mediating an initial low-affinity interaction that is subsequently stabilized by a conformational change in the complex to an "open" form (partly due to phosphorylation of μ2 itself) (33) that exposes the C-terminal two-thirds of μ2 and allows it to bind *YXXϕ* signals in transmembrane protein cargo and another molecule of PIP_2. Conceivably, the Serinc3 PSAC might partly substitute for PIP_2 in this scenario, stabilizing the interaction between AP-2, the lipid bilayer, and the transmembrane protein cargo, here Serinc3 itself. Fig. 7 depicts a schematic representation of how the PSACs in Serinc3 and furin could interact with AP-2, which is shown in an open conformation with a TGN38-derived peptide bound to μ2 at the *YXXϕ*-binding site (23).

We previously reported that the sites in *serinc3* at which the human gene encodes serines of the putative PSAC in loop 10 (positions 380 and 383) are under positive (or diversifying) selection when nonhuman primate nucleotide sequences are compared (32). This genetic phenomenon is often the signature of a host–pathogen conflict, in which the host antiviral gene is subject to selection pressure to escape the ability of viral proteins to antagonize it (24). Thus, we remain intrigued that the ability of Serinc3 to bind μ2 via the PSAC in loop 10 appears to wax and wane over the phylogeny of placental mammals. Whereas the Nef protein of HIV-1 antagonizes the inhibitory effects of Serinc family proteins on viral infectivity (21, 22), this function is provided by the transmembrane protein glycoGag in murine leukemia virus (an oncogenic retrovirus) and by the S2 protein in equine infectious anemia virus (a lentivirus of horses) (34, 35). In neither the mouse nor the horse is the PSAC signal intact; in the mouse, the serines are replaced by asparagines, and in the horse, they are replaced by glycines. Because these viral antagonists of the Serinc proteins presumably function by affecting membrane trafficking, whether the presence or absence of an intact PSAC motif in Serinc proteins affects their activity remains an interesting and open question. So far, we have shown only that the presence or absence of an intact PSAC has no influence on the activity of a single HIV-1 Nef protein as an antagonist of Serinc3, even though the analogous cytoplasmic loop has recently been shown to be a determinant of the susceptibility of Serinc5 to Nef proteins (36).

Although the role of the furin PSAC in endocytosis is well-supported (4), we have so far been unable to support a similar role for the putative PSAC in Serinc3. Conceivably, despite the apparent specificity of the Serinc3 loop 10–μ2 interaction (its dependence on the loop 10 serines and on basic region 4 of μ2), this *in vitro* interaction might not have biological relevance, or alternatively, its functional relevance might be lost when the protein is overexpressed. The Serincs appear to be relatively low-abundance proteins, and during our human cell–based experiments, we suspect that the protein is expressed well above physiological levels. We are aware of no reagents able to detect endogenous Serincs; indeed, the only data regarding endogenous Serinc3 derive from cytoplasmic fractionation studies using HeLa cells and MS (37). Those data suggest that

endogenous Serinc3 is endosomal and that its endosomal distribution is modulated by AP-4, an AP family member with relatively poorly characterized function. Conceivably, the μ subunit of AP-4 could be the biologically relevant binding partner of the Serinc3 loop 10 PSAC, a hypothesis that we aim to test.

Recently, a haploid cell genetic screen using a gene-disrupting retrovirus and a fusion protein of CD8 and the CD of furin (mutated to lack its Y*XXϕ* signal) as a flow cytometric indicator revealed that μ1 is a target of the PSAC in furin (20), a conclusion fully consistent with the data herein. These investigators also reported that basic region 2 of μ1, the site that interacts with the acidic cluster of Nef, is required for the interaction of the furin CD with μ1 *in vitro*; this result is potentially but not necessarily at odds with the data herein, in which the analogous region of μ2 appears dispensable, although modestly contributory, for binding to the furin CD. Nonetheless, the authors found that whereas a μ1 mutant in which basic region 2 was disrupted did not fully support the modulation of class I MHC by Nef, it paradoxically fully supported the trafficking of furin (*i.e.* basic region 2 of μ1 was dispensable for furin trafficking) (20). Conceivably, the presence of additional AP binding signals in the CD of furin could resolve this paradox, leading to the authors' notion that redundancies in the sorting signals within the CDs of cellular proteins might render them less susceptible to disruption than the single binding sites in viral proteins (20). Another possibility, supported by the data herein, is that the interaction of the furin CD with μ2 is a key determinant of furin trafficking.

Along a distinct line of reasoning, our data suggest that multiple basic regions on the μ subunits can be utilized differentially by the PSACs of different viral and cellular proteins. This scenario offers the potential to inhibit the interaction of viral proteins such as Nef and Vpu with specific basic regions on the μ subunits (namely regions 1 and 2 herein), while leaving the trafficking of at least some cellular proteins, such as furin and Serinc3, relatively unaffected. Exactly how that might be accomplished awaits a high-resolution structural definition of these interactions.

Materials and methods

Plasmids and human cell lines

The HeLa-derived reporter cell line P4.R5 (38) was obtained through the NIH AIDS Reagent Program (Division of AIDS, NIAID, National Institutes of Health) from Nathaniel Landau. The cells were maintained in Dulbecco's modified Eagle's medium supplemented with 10% fetal bovine serum, penicillin/streptomycin, and 1 μg/ml puromycin. The double-knockout Jurkat TAg T lymphoid cell line in which the *SERINC3* and *SERINC5* ORFs are disrupted was a kind gift from Heinrich Göttlinger (22) and was maintained in RPMI medium supplemented with 10% fetal bovine serum and penicillin/streptomycin.

The proviral plasmids pNL4-3 and pNL4-3ΔNef have been described previously (39–41). The expression plasmid encoding a C-terminally HA epitope–tagged SERINC3 in the modified mammalian expression vector pBJ6 was a kind gift from Massimo Pizzato (21). The SERINC3-HA coding sequence was transferred to a pBJ5 expression vector by restriction digestion and ligation using NotI and EcoRI sites. Expression plasmids encoding pBJ5-SERINC3 ΔSDEED, ADEED, and SAAAA were generated by site-directed mutagenesis using a QuikChange II site-directed mutagenesis kit (Agilent Technologies); primers were synthesized by Integrated DNA Technologies.

Cloning, expression, and purification of recombinant proteins

The HIV1-Vpu, furin, and Serinc3 constructs were designed based on their known or predicted cytoplasmic domains. The CDs of Vpu (residues 28–81) and furin (residues 739–794) were cloned into the pGEX4T1 vector, which added a GST tag at the N terminus of the protein. We used computational predictions to identify the topology of Serinc3 and its putative extracellular and intracellular loops. Loop 10 of Serinc3 (residues 354–404) is predicted to be cytoplasmic, and by sequence inspection it contains a potential PSAC motif, ^{383}SDEED^{387}, which represents a consensus CK-II site. We cloned this loop into the pGEX4T1 vector. For the AP-1 and AP-2 medium subunits (μ1 and μ2), we used previously created (12) truncated versions of μ1 (residues 158–423) and μ2 (residues 159–435) in the pMAT9s vector, in which the μ sequences are fused to that of MBP. For reverse pulldown studies, we created MBP-μ2(159–435)-GST and MBP-Serinc3(355–405) constructs. The GST tag was added to the C terminus of a previously created MBP-μ2CTD construct with a tobacco etch virus protease cut site between μ2CTD and GST in the pMAT9s vector. MBP-SERINC3(355–405) constructs were prepared similarly with a SARS M^{pro}-cleavable (42, 43) His_6 tag at the C terminus in the pMAT9s vector; these constructs were cloned using ligation-independent Gibson assembly.

The GST-tagged Vpu, furin, Serinc3-loop 10, and MBP-tagged Serinc3-loop 10 proteins were expressed in BL21(DE3) competent cells (New England Biolabs). Protein expression was induced with 0.1 mM isopropyl β-D-thiogalactopyranoside at A_{600} of 0.6–0.8 at 16 °C overnight. To make phosphorylated proteins, the GST fusions were co-expressed with the α and β subunits of CK-II cloned into the pCDFDuet vector. MBP-μ1, MBP-μ2, and MBP-μ2-GST proteins were co-expressed with the pGro7 chaperone vector(44, 45) and additionally induced with 1.5 g/liter medium L-(+)-arabinose at A_{600} ~0.2. Cell pellets were resuspended in appropriate binding buffers and lysed either by a French press homogenizer or by micofluidization. Lysates were clarified by centrifugation at 14,000 rpm. GST-Vpu, GST-furin, and GST-Serinc3 were purified by GST-affinity, HiPrep Q anion-exchange, and S200pg chromatography. MBP-μ1 and MBP-μ2 proteins were purified by His-select nickel-affinity gel, HiPrep S cation-exchange, and S200pg chromatography. MBP-μ2CTD-GST was purified using Ni-NTA-agarose, followed by a GST affinity column and gel filtration chromatography on a Superdex 200 prep-grade column. MBP-SERINC3 lysate was supplemented with 10 mM NaF and purified by Ni-NTA, HiTrap Q anion-exchange chromatography, and S200pg chromatography.

All mutations in furin, Serinc3, and μ2 were generated using the QuikChange mutagenesis kit (Agilent Technologies, La Jolla, CA). Mutant proteins were expressed and purified as described above.

Analysis of phosphorylation by LC/MS

GST-Serinc3 protein was co-expressed with CK-II in BL21 (DE3) cells, and purified samples were analyzed by LC/MS as follows.

In-solution protein digestion—Samples (95 μg in 5.0 μl of Tris buffer including 2 mM DTT) were denatured by the addition of 5.0 μl of 8 M urea, 0.4 M ammonium bicarbonate. The proteins were reduced by the addition of 1.0 μl of 45 mM DTT (Pierce Thermo Scientific) and incubation at 37 °C for 30 min and then alkylated with the addition of 1.25 μl of 100 mM iodoacetamide (Sigma-Aldrich) with incubation in the dark at room temperature for 30 min. The urea concentration was adjusted to 2 M by the addition of 7.75 μl of water. Samples were then enzymatically digested with 2.0 μg of trypsin (Promega sequencing grade modified trypsin) and incubation at 37 °C for 16 h. Samples were desalted using C18 MacroSpin columns (Nest Group) following the manufacturer's directions with peptides eluted with 0.1% TFA, 80% acetonitrile. Eluted samples were dried and dissolved in MS loading buffer (2% acetonitrile, 0.2% TFA). A Nanodrop (Thermo Scientific Nanodrop 2000 UV-visible spectrophotometer) was used to measure the protein concentrations (A_{260}/A_{280}). An aliquot of each sample was then diluted with MS loading buffer to 0.02 μg/μl, with 0.1 μg (5 μl) injected for LC-MS/MS analysis.

LC-MS/MS—LC-MS/MS analysis was performed on a Thermo Scientific Q Exactive Plus mass spectrometer equipped with a Waters nanoAcquity UPLC system utilizing a binary solvent system (Buffer A: 100% water, 0.1% formic acid; Buffer B: 100% acetonitrile, 0.1% formic acid). Trapping was performed at 5 μl/min, 97% Buffer A for 3 min using a Waters Symmetry® C18 180 μm × 20-mm trap column. Peptides were separated using an ACQUITY UPLC PST (BEH) C18 nanoACQUITY column 1.7 μm, 75 μm × 250 mm (37 °C) and eluted at 300 nl/min with the following gradient: 3% buffer B at initial conditions; 5% B at 1 min; 35% B at 50 min; 50% B at 60 min; 90% B at 65 min; 90% B at 70 min; return to initial conditions at 71 min. MS was acquired in profile mode over the 300–1,700 *m*/*z* range using one microscan, 70,000 resolution, AGC target of 3E6, and a maximum injection time of 45 ms. Data-dependent MS/MS spectra were acquired in centroid mode on the top 20 precursors per MS scan using one microscan, 17,500 resolution, AGC target of 1E5, maximum injection time of 100 ms, and an isolation window of 1.7 *m*/*z*. Precursors were fragmented by higher-energy collisional dissociation activation with a collision energy of 28%. MS/MS data were collected on species with an intensity threshold of 2E4, charge states 2–6, and peptide match preferred. Dynamic exclusion was set to 20 s.

Peptide identification—Data were analyzed using Proteome Discoverer software (version 1.3, Thermo Scientific) and searched in house using the Mascot algorithm (version 2.6.0) (Matrix Science). The data were searched against a custom database containing the constructs of interest as well as the SwissProtein database with taxonomy restricted to *E. coli*. Search parameters included trypsin digestion with up to two missed cleavages, peptide mass tolerance of ±10 ppm, MS/MS fragment tolerance of ±0.02 Da, fixed modification of carbamidomethyl cysteine, and variable modifications of methionine oxidation and phosphorylation on serine, threonine, and tyrosine. Normal and decoy database searches were run, with the confidence level set to 95% ($p < 0.05$).

Phospho-tag gel assay

CK-II–mediated *in vitro* phosphorylation of Vpu, furin, and Serinc3 was checked by Phospho-tag phosphoprotein gel stain (Genecopoeia, Rockville, MD) using the vendor-provided protocol. In brief, equal amounts of proteins that were expressed either with or without CK-II were run on an SDS-polyacrylamide gel, which was fixed with a solution of 50% methanol, 10% acetic acid and then washed in water before staining with the Phos-tag phosphoprotein gel stain for 90 min. After destaining and washing according to the manufacturer's instructions, the gel was imaged using a 300-nm UV transilluminator.

GST pulldown assays

Purified GST-furin, GST-Serinc3, and MBP-μ1/MBP-μ2 proteins were used for *in vitro* GST pulldown. An equimolar ratio of these proteins was mixed with GST-resin and incubated overnight at 4 °C. The next day, the GST resins were extensively washed with buffer containing 20 mM Tris-HCl, pH 7.5, and 150 mM NaCl to remove the unbound proteins. The bound proteins were eluted with 10 mM GSH reduced in 50 mM Tris-HCl, pH 8.0. The formation of protein–protein complexes between GST-furin or GST-Serinc3 and MBP-μ1 or MBP-μ2 were detected by SDS-PAGE using Coomassie Blue stain. For "reverse" GST pulldown assays, MBP-μ2CTD-GST (0.45 mg) and MBP-SERINC3 and related mutants (~1 mg, 5-fold molar excess) were mixed in a final volume of 100 μl. Reaction mixtures were loaded onto small, gravity flow columns containing 0.5 ml of GSH-Sepharose 4B resin (GE Healthcare). The resin was extensively washed with 4 × 750 μl of GST binding buffer (50 mM Tris, pH 8, 100 mM NaCl, 0.1 mM tris(2-carboxyethyl) phosphine). Bound protein complexes were eluted with 4 × 250 μl of GST elution buffer containing 10 mM reduced GSH. Eluted proteins were analyzed by SDS-PAGE and stained with Coomassie Blue.

Size-exclusion chromatography

The formation of stable protein complexes between the GST-fused CDs of Vpu, furin, and Serinc3-L10 and MBP-μ2 was assessed by SEC. A Superose 6 10/300GL (GE Healthcare) small-scale SEC column was used with an AKTA Pure chromatography system. The column was pre-equilibrated with buffer containing 20 mM Tris-HCl, pH 7.5, 150 mM NaCl, 10% glycerol, 2 mM DTT, and 5 mM EDTA. The two purified protein components (the GST fusions and MBP-μ2) were mixed in an equimolar ratio in a total volume of 100 μl, incubated at 4 °C for 1 h, and then injected into the SEC column. The eluting protein was detected by UV absorbance at 280 nM. Molecular weight estimates for the peak fractions were derived using gel-filtration standards of various sizes. The peak fractions were analyzed by SDS-PAGE.

Biolayer interferometry

Binding affinities between phosphorylated GST-Vpu, -furin, and -Serinc3 with MBP-μ2 were determined by biolayer interferometry on an Octet Red instrument (ForteBio). His-tagged MBP-μ2 was immobilized on Ni-NTA capture sensors (ForteBio). The CDs of Vpu, furin, and Serinc3, each fused to GST, were assessed as free analytes in solution (PBS at pH 7.4). For measurement of the kinetic parameters, the analytes were serially diluted to five different concentrations, as shown in Fig. 3. The data were analyzed using the ForteBio analysis software version 7.1, and the kinetic parameters were calculated using a global fit 1:1 model, yielding the association (k_{on}), dissociation (k_{off}), and affinity constants (k_d) for each interaction.

Phylogenetic analyses

To test whether evolution at sites 380 and 383 co-evolved with each other, we employed a Bayesian graphical model using the Spidermonkey (46) package. The relationship between the two sites was explored using a one-parent network conditioned on a maximum likelihood phylogeny inferred using IQ-Tree (47) under a GTR + Γ_4 substitution model.

HIV-1 infectivity assays

To determine the effect of SERINC3 mutations on the restriction of HIV-1 infectivity and Nef responsiveness, 3.75×10^5 Jurkat TAg (−*SERINC3*/−*SERINC5*) cells were co-transfected with either 1.15 μg of pNL4-3 or pNL4-3ΔNef proviral plasmid and 100 ng of plasmid encoding WT or mutant SERINC3, using DNA-In Jurkat transfection reagent (MTI GlobalStem). Two days later, the suspension cells were pelleted by low-speed centrifugation, and virions were partially purified from the culture supernatants by ultracentrifugation at 20,000 × *g* through a 20% sucrose cushion. The viral pellets were resuspended in Dulbecco's modified Eagle's medium supplemented with 10% fetal bovine serum, and infectivity was determined by infecting 2×10^4 HeLa P4.R5 cells in a 48-well plate in duplicate with serial dilutions of the virion preparations. Two days after infection, the cells were fixed and stained for β-gal activity, and the number of infectious centers was measured by computer-assisted image analysis as described previously (48). The data are expressed as the number of infectious centers normalized to the concentration of HIV capsid antigen (p24), as measured by ELISA (ABL, Rockville, MD).

Immunoblotting

Cell lysates and virion pellets from infectivity experiments were analyzed by SDS-PAGE and Western blotting. The viral and cell pellets were resuspended in Laemmli buffer supplemented with 50 mM tris(2-carboxyethyl)phosphine. Cell samples were sonicated before SDS-PAGE and Western blotting. Western blots were probed for exogenous SERINC3 expression using mouse anti-HA (HA.11, clone 16B12, Biolegend). The blots were also probed using mouse anti-GAPDH (Genentech) as a cellular protein loading control and mouse anti-p24 (EMD Millipore) as a virion-protein loading control. Horseradish peroxidase–conjugated goat anti-mouse IgG (Bio-Rad) was used as a secondary antibody, and the immunoreactive bands were visualized by enhanced chemiluminescence. Protein band intensities were measured using Bio-Rad ImageLab software (version 5.1).

Author contributions—R. S., C. S., C. L., J. Guenaga, R. W., J. O. W., X. J., Y. X., and J. Garcia designed and/or performed the experiments. All authors interpreted the data and edited or wrote the manuscript.

Acknowledgments—We thank Marissa Suarez for the p24 ELISAs, Massimo Pizzato for the C-terminally HA epitope–tagged SERINC3 in the expression vector pBJ6, and Heinrich Göttlinger for the Jurkat TAg serinc3/5 knockout cells.

References

1. Bonifacino, J. S., and Traub, L. M. (2003) Signals for sorting of transmembrane proteins to endosomes and lysosomes. *Annu. Rev. Biochem.* **72,** 395–447 CrossRef Medline
2. Robinson, M. S. (2004) Adaptable adaptors for coated vesicles. *Trends Cell Biol.* **14,** 167–174 CrossRef Medline
3. Owen, D. J., Collins, B. M., and Evans, P. R. (2004) Adaptors for clathrin coats: structure and function. *Annu. Rev. Cell Dev. Biol.* **20,** 153–191 CrossRef Medline
4. Voorhees, P., Deignan, E., van Donselaar, E., Humphrey, J., Marks, M. S., Peters, P. J., and Bonifacino, J. S. (1995) An acidic sequence within the cytoplasmic domain of furin functions as a determinant of trans-Golgi network localization and internalization from the cell surface. *EMBO J.* **14,** 4961–4975 Medline
5. Owen, D. J., and Evans, P. R. (1998) A structural explanation for the recognition of tyrosine-based endocytotic signals. *Science* **282,** 1327–1332 CrossRef Medline
6. Kelly, B. T., McCoy, A. J., Späte, K., Miller, S. E., Evans, P. R., Höning, S., and Owen, D. J. (2008) A structural explanation for the binding of endocytic dileucine motifs by the AP2 complex. *Nature* **456,** 976–979 CrossRef Medline
7. Crump, C. M., Xiang, Y., Thomas, L., Gu, F., Austin, C., Tooze, S. A., and Thomas, G. (2001) PACS-1 binding to adaptors is required for acidic cluster motif-mediated protein traffic. *EMBO J.* **20,** 2191–2201 CrossRef Medline
8. Teuchert, M., Schäfer, W., Berghöfer, S., Hoflack, B., Klenk, H. D., and Garten, W. (1999) Sorting of furin at the trans-Golgi network: interaction of the cytoplasmic tail sorting signals with AP-1 Golgi-specific assembly proteins. *J. Biol. Chem.* **274,** 8199–8207 CrossRef Medline
9. Ghosh, P., and Kornfeld, S. (2004) The cytoplasmic tail of the cation-independent mannose 6-phosphate receptor contains four binding sites for AP-1. *Arch. Biochem. Biophys.* **426,** 225–230 CrossRef Medline
10. Noviello, C. M., Benichou, S., and Guatelli, J. C. (2008) Cooperative binding of the class I major histocompatibility complex cytoplasmic domain and human immunodeficiency virus type 1 Nef to the endosomal AP-1 complex via its μ subunit. *J. Virol.* **82,** 1249–1258 CrossRef Medline
11. Singh, R. K., Lau, D., Noviello, C. M., Ghosh, P., and Guatelli, J. C. (2009) An MHC-I cytoplasmic domain/HIV-1 Nef fusion protein binds directly to the μ subunit of the AP-1 endosomal coat complex. *PLoS One* **4,** e8364 CrossRef Medline
12. Jia, X., Singh, R., Homann, S., Yang, H., Guatelli, J., and Xiong, Y. (2012) Structural basis of evasion of cellular adaptive immunity by HIV-1 Nef. *Nat. Struct. Mol. Biol.* **19,** 701–706 CrossRef Medline
13. Willey, R. L., Maldarelli, F., Martin, M. A., and Strebel, K. (1992) Human immunodeficiency virus type 1 Vpu protein induces rapid degradation of CD4. *J. Virol.* **66,** 7193–7200 Medline
14. Van Damme, N., Goff, D., Katsura, C., Jorgenson, R. L., Mitchell, R., Johnson, M. C., Stephens, E. B., and Guatelli, J. (2008) The interferon-induced protein BST-2 restricts HIV-1 release and is downregulated from the cell surface by the viral Vpu protein. *Cell Host Microbe* **3,** 245–252 CrossRef Medline

15. Shah, A. H., Sowrirajan, B., Davis, Z. B., Ward, J. P., Campbell, E. M., Planelles, V., and Barker, E. (2010) Degranulation of natural killer cells following interaction with HIV-1-infected cells is hindered by down-modulation of NTB-A by Vpu. *Cell Host Microbe* **8,** 397–409 CrossRef Medline
16. Ramirez, P. W., Famiglietti, M., Sowrirajan, B., DePaula-Silva, A. B., Rodesch, C., Barker, E., Bosque, A., and Planelles, V. (2014) Downmodulation of CCR7 by HIV-1 Vpu results in impaired migration and chemotactic signaling within $CD4^+$ T cells. *Cell Rep.* **7,** 2019–2030 CrossRef Medline
17. Stoneham, C. A., Singh, R., Jia, X., Xiong, Y., and Guatelli, J. (2017) Endocytic activity of HIV-1 Vpu: phosphoserine-dependent interactions with clathrin adaptors. *Traffic* **18,** 545–561 CrossRef Medline
18. Margottin, F., Bour, S. P., Durand, H., Selig, L., Benichou, S., Richard, V., Thomas, D., Strebel, K., and Benarous, R. (1998) A novel human WD protein, h-β TrCp, that interacts with HIV-1 Vpu connects CD4 to the ER degradation pathway through an F-box motif. *Mol. Cell* **1,** 565–574 CrossRef Medline
19. Hirst, J., and Robinson, M. S. (1998) Clathrin and adaptors. *Biochim. Biophys. Acta* **1404,** 173–193 CrossRef Medline
20. Navarro Negredo, P., Edgar, J. R., Wrobel, A. G., Zaccai, N. R., Antrobus, R., Owen, D. J., and Robinson, M. S. (2017) Contribution of the clathrin adaptor AP-1 subunit micro1 to acidic cluster protein sorting. *J. Cell Biol.* **216,** 2927–2943 Medline
21. Rosa, A., Chande, A., Ziglio, S., De Sanctis, V., Bertorelli, R., Goh, S. L., McCauley, S. M., Nowosielska, A., Antonarakis, S. E., Luban, J., Santoni, F. A., and Pizzato, M. (2015) HIV-1 Nef promotes infection by excluding SERINC5 from virion incorporation. *Nature* **526,** 212–217 CrossRef Medline
22. Usami, Y., Wu, Y., and Göttlinger, H. G. (2015) SERINC3 and SERINC5 restrict HIV-1 infectivity and are counteracted by Nef. *Nature* **526,** 218–223 CrossRef Medline
23. Jackson, L. P., Kelly, B. T., McCoy, A. J., Gaffry, T., James, L. C., Collins, B. M., Höning, S., Evans, P. R., and Owen, D. J. (2010) A large-scale conformational change couples membrane recruitment to cargo binding in the AP2 clathrin adaptor complex. *Cell* **141,** 1220–1229 CrossRef Medline
24. Daugherty, M. D., and Malik, H. S. (2012) Rules of engagement: molecular insights from host-virus arms races. *Annu. Rev. Genet.* **46,** 677–700 CrossRef Medline
25. Kueck, T., Foster, T. L., Weinelt, J., Sumner, J. C., Pickering, S., and Neil, S. J. (2015) Serine phosphorylation of HIV-1 Vpu and its binding to tetherin regulates interaction with clathrin adaptors. *PLoS Pathog.* **11,** e1005141 CrossRef Medline
26. Kueck, T., and Neil, S. J. (2012) A cytoplasmic tail determinant in HIV-1 Vpu mediates targeting of tetherin for endosomal degradation and counteracts interferon-induced restriction. *PLoS Pathog.* **8,** e1002609 CrossRef Medline
27. Jia, X., Weber, E., Tokarev, A., Lewinski, M., Rizk, M., Suarez, M., Guatelli, J., and Xiong, Y. (2014) Structural basis of HIV-1 Vpu-mediated BST2 antagonism via hijacking of the clathrin adaptor protein complex 1. *Elife* **3,** e02362 CrossRef Medline
28. Schubert, U., Henklein, P., Boldyreff, B., Wingender, E., Strebel, K., and Porstmann, T. (1994) The human immunodeficiency virus type 1 encoded Vpu protein is phosphorylated by casein kinase-2 (CK-2) at positions Ser52 and Ser56 within a predicted α-helix-turn-α-helix-motif. *J. Mol. Biol.* **236,** 16–25 CrossRef Medline
29. Jones, B. G., Thomas, L., Molloy, S. S., Thulin, C. D., Fry, M. D., Walsh, K. A., and Thomas, G. (1995) Intracellular trafficking of furin is modulated by the phosphorylation state of a casein kinase II site in its cytoplasmic tail. *EMBO J.* **14,** 5869–5883 Medline
30. Rohde, G., Wenzel, D., and Haucke, V. (2002) A phosphatidylinositol (4,5)-bisphosphate binding site within μ2-adaptin regulates clathrin-mediated endocytosis. *J. Cell Biol.* **158,** 209–214 CrossRef Medline
31. Höning, S., Ricotta, D., Krauss, M., Späte, K., Spolaore, B., Motley, A., Robinson, M., Robinson, C., Haucke, V., and Owen, D. J. (2005) Phosphatidylinositol-(4,5)-bisphosphate regulates sorting signal recognition by the clathrin-associated adaptor complex AP2. *Mol. Cell* **18,** 519–531 CrossRef Medline
32. Murrell, B., Vollbrecht, T., Guatelli, J., and Wertheim, J. O. (2016) The evolutionary histories of antiretroviral proteins SERINC3 and SERINC5 do not support an evolutionary arms race in primates. *J. Virol.* **90,** 8085–8089 CrossRef Medline
33. Conner, S. D., and Schmid, S. L. (2002) Identification of an adaptor-associated kinase, AAK1, as a regulator of clathrin-mediated endocytosis. *J. Cell Biol.* **156,** 921–929 CrossRef Medline
34. Usami, Y., Popov, S., and Göttlinger, H. G. (2014) The Nef-like effect of murine leukemia virus glycosylated gag on HIV-1 infectivity is mediated by its cytoplasmic domain and depends on the AP-2 adaptor complex. *J. Virol.* **88,** 3443–3454 CrossRef Medline
35. Chande, A., Cuccurullo, E. C., Rosa, A., Ziglio, S., Carpenter, S., and Pizzato, M. (2016) S2 from equine infectious anemia virus is an infectivity factor which counteracts the retroviral inhibitors SERINC5 and SERINC3. *Proc. Natl. Acad. Sci. U.S.A.* **113,** 13197–13202 CrossRef Medline
36. Dai, W., Usami, Y., Wu, Y., and Göttlinger, H. (2018) A long cytoplasmic loop governs the sensitivity of the anti-viral host protein SERINC5 to HIV-1 Nef. *Cell Rep.* **22,** 869–875 CrossRef Medline
37. Davies, A. K. I., DN; Edgar, J. R., Archuleta, T. L., Hirst, J., Jackson, L. P., Robinson, M. S., and Borner, G. H. H. (2017) AP-4 vesicles unmasked by organellar proteomics to reveal their cargo and machinery. *bioRxiv* CrossRef
38. Charneau, P., Mirambeau, G., Roux, P., Paulous, S., Buc, H., and Clavel, F. (1994) HIV-1 reverse transcription. A termination step at the center of the genome. *J. Mol. Biol.* **241,** 651–662 CrossRef Medline
39. Adachi, A., Gendelman, H. E., Koenig, S., Folks, T., Willey, R., Rabson, A., and Martin, M. A. (1986) Production of acquired immunodeficiency syndrome-associated retrovirus in human and nonhuman cells transfected with an infectious molecular clone. *J. Virol.* **59,** 284–291 Medline
40. Spina, C. A., Kwoh, T. J., Chowers, M. Y., Guatelli, J. C., and Richman, D. D. (1994) The importance of nef in the induction of human immunodeficiency virus type 1 replication from primary quiescent CD4 lymphocytes. *J. Exp. Med.* **179,** 115–123 CrossRef Medline
41. Chowers, M. Y., Spina, C. A., Kwoh, T. J., Fitch, N. J., Richman, D. D., and Guatelli, J. C. (1994) Optimal infectivity *in vitro* of human immunodeficiency virus type 1 requires an intact nef gene. *J. Virol.* **68,** 2906–2914 Medline
42. Xue, X., Yang, H., Shen, W., Zhao, Q., Li, J., Yang, K., Chen, C., Jin, Y., Bartlam, M., and Rao, Z. (2007) Production of authentic SARS-CoV M^{pro} with enhanced activity: application as a novel tag-cleavage endopeptidase for protein overproduction. *J. Mol. Biol.* **366,** 965–975 CrossRef Medline
43. Xue, X., Yu, H., Yang, H., Xue, F., Wu, Z., Shen, W., Li, J., Zhou, Z., Ding, Y., Zhao, Q., Zhang, X. C., Liao, M., Bartlam, M., and Rao, Z. (2008) Structures of two coronavirus main proteases: implications for substrate binding and antiviral drug design. *J. Virol.* **82,** 2515–2527 CrossRef Medline
44. Nishihara, K., Kanemori, M., Kitagawa, M., Yanagi, H., and Yura, T. (1998) Chaperone coexpression plasmids: differential and synergistic roles of DnaK-DnaJ-GrpE and GroEL-GroES in assisting folding of an allergen of Japanese cedar pollen, Cryj2, in *Escherichia coli*. *Appl. Environ. Microbiol.* **64,** 1694–1699 Medline
45. Thomas, J. G., Ayling, A., and Baneyx, F. (1997) Molecular chaperones, folding catalysts, and the recovery of active recombinant proteins from *E. coli*: to fold or to refold. *Appl. Biochem. Biotechnol.* **66,** 197–238 CrossRef Medline
46. Poon, A. F., Lewis, F. I., Frost, S. D., and Kosakovsky Pond, S. L. (2008) Spidermonkey: rapid detection of co-evolving sites using Bayesian graphical models. *Bioinformatics* **24,** 1949–1950 CrossRef Medline
47. Nguyen, L. T., Schmidt, H. A., von Haeseler, A., and Minh, B. Q. (2015) IQ-TREE: a fast and effective stochastic algorithm for estimating maximum-likelihood phylogenies. *Mol. Biol. Evol.* **32,** 268–274 CrossRef Medline
48. Day, J. R., Martínez, L. E., Sásik, R., Hitchin, D. L., Dueck, M. E., Richman, D. D., and Guatelli, J. C. (2006) A computer-based, image-analysis method to quantify HIV-1 infection in a single-cycle infectious center assay. *J. Virol. Methods* **137,** 125–133 CrossRef Medline
49. Robert, X., and Gouet, P. (2014) Deciphering key features in protein structures with the new ENDscript server. *Nucleic Acids Res.* **42,** W320–W324 CrossRef Medline